

Laser induced proton acceleration by resonant nano-rod antenna for fusion

István Papp^{1,2}, Larissa Bravina⁴, Mária Csete^{1,5}, Archana Kumari^{1,2}, Igor N. Mishustin⁶, Anton Motornenko⁶, Péter Rácz^{1,2}, Leonid M. Satarov⁶, Horst Stöcker^{6,7,8}, András Szenes^{1,5}, Dávid Vass^{1,5}, Tamás S. Biró^{1,2}, László P. Csernai^{1,2,3,9}, Norbert Kroó^{1,2,10}

(part of NAPLIFE Collaboration)

- ¹ *Wigner Research Centre for Physics, Budapest, Hungary*
² *Hungarian Bureau for Research Development and Innovation*
³ *Dept. of Physics and Technology, University of Bergen, 5007 Bergen, Norway*
⁴ *Department of Physics, University of Oslo, Norway*
⁵ *Dept. of Optics and Quantum Electronics, Univ. of Szeged, Hungary*
⁶ *Frankfurt Institute for Advanced Studies, 60438 Frankfurt/Main, Germany*
⁷ *Inst. für Theoretische Physik, Goethe Universität Frankfurt, 60438 Frankfurt/Main, Germany*
⁸ *GSI Helmholtzzentrum für Schwerionenforschung GmbH, 64291 Darmstadt, Germany*
⁹ *Csernai Consult Bergen, Bergen, Norway*
¹⁰ *Hungarian Academy of Sciences, 1051 Budapest, Hungary*

Recently laser induced fusion with simultaneous volume ignition, a spin-off from relativistic heavy ion collisions, was proposed, where implanted nano antennas regulated and amplified the light absorption in the fusion target. Studies of resilience of the nano antennas were published recently in vacuum and in UDMA-TEGDMA medium. These studies concluded that the lifetime of the plasmonic effect is longer in medium, however, less energy was observed in the UDMA-TEGDMA copolymer, due to the smaller resonant size of gold nanoantenna than in case of Vacuum. Here we show how the plasmonic effect behaves in an environment fully capable of ionization, surrounded by Hydrogen atoms close to liquid densities. We performed numerical simulations treating the electrons of gold in the conduction band as strongly coupled plasma. The results show that the protons close to the nanorod's surface follow the collectively moving electrons rather than the incoming electric field of the light. The results also show that the plasmonic accelerating effect is also dependent on the laser intensity.

I. INTRODUCTION

In recent years, NANOPlasmonic Laser Inertial Fusion Experiments (NAPLIFE) [1] were proposed to achieve in an improved way nuclear fusion as a clean and efficient source of energy. The aim is to achieve laser driven fusion in a non-thermal, collider configuration to avoid instabilities during ignition. Simultaneous volume (or "time-like") ignition [5, 6] can be achieved with enhanced energy absorption with the help of nano antennas implanted into the target material [7]. This should prevent the development of the mechanical Rayleigh-Taylor instability. Furthermore, the nuclear burning should not propagate from a central hot spot to the outside edge as the ignition is simultaneous in the whole target volume.

However, before this approach can be put into practice, it is crucial to understand the resilience of these nano antennas under various conditions. To this end, recent studies have been conducted to investigate the behavior of the nano antennas in vacuum [23] as well as in a UDMA-TEGDMA medium. These studies provide valuable insights into the behavior of the nano antennas and their potential as a key element in achieving laser

induced fusion with simultaneous volume ignition.

Non-equilibrium and linear colliding configuration have been introduced already [12, 13]. Here we study the idea of layered flat target fuel with embedded nanorod antennas, that regulate laser light absorption to enforce simultaneous ignition. We plan a seven-layer flat target with different nanorod densities. [14, 16, 17]. In order to prepare such a layered target, the ignition fuel (e.g. deuterium, D, tritium, T, or other nuclei for fusion) are embedded into a hard thin polymer material of seven, $3\mu\text{m}$ thick layers. These polymers are Urethane Dimethacrylate (UDMA) and Triethylene glycol dimethacrylate (TEGDMA) in (3:1) mass ratio [18, 19].

The linear colliding beam configuration allows for a much simpler flat target configuration [1, 16], utilizing a non-equilibrium, ignition dynamics. This is realized by relativistic collisions of two target slabs, produced by using the Laser Wake Field Acceleration (LWFA) mechanism [34]. The use of femtosecond laser pulses leads to rapid ignition with high, beam-directed collision velocities.

The benefits of non-equilibrium configuration were first introduced in ref. [12], and experimentally tested in lin-

ear colliding configuration [13]. Similar pre-compression was reached by this configuration as in the National Ignition Facility (NIF).

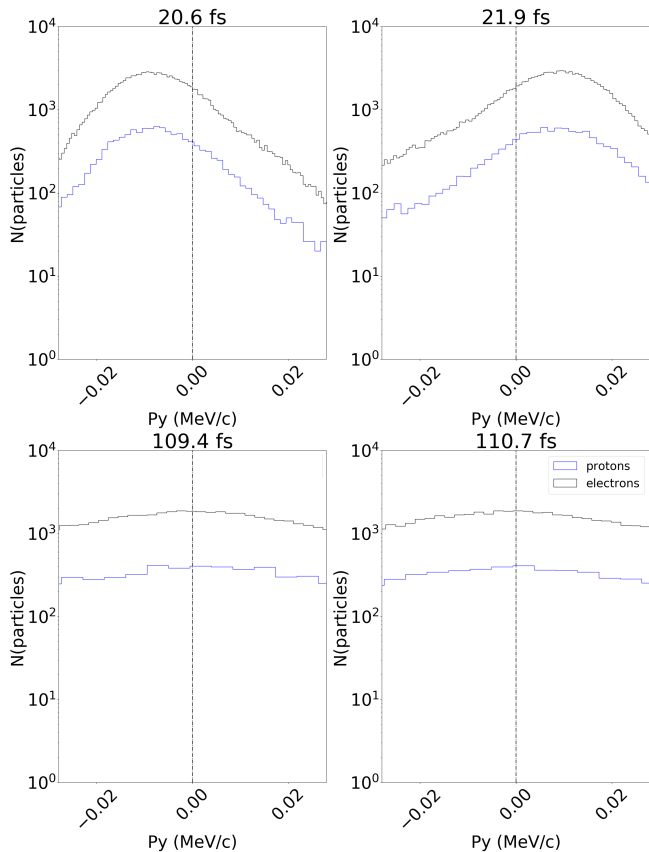


FIG. 1. (color online) A snapshot of pairs of particle number oscillations half of a period ($T/2$) apart are shown at an earlier (top) and later (bottom) stage. The histogram of the y directed momentum distribution is shown. Black lines show momentum distribution of the electron marker particles, while black lines show protons surrounding the nanorod. Vertical line in the middle separates particles going up (right) and down (left) along the nano antenna. The highest peak of the proton momentum distribution is not in total anti-phase of the highest peak of the electrons, they follow the electrons with a small delay. This suggests that the protons are moved not by the electric field of the laser beam but in the near field of the Localized Surface Plasmon Polaritons. The widening of the momentum distribution can be attributed to the kinetic model assumption, where both the conduction and binding electrons are considered freely movable. The resonance of the nanorod has a period of $T = 2.65$ fs.

In addition to achieving simultaneous energy deposition there are other significant effects in the NAPLIFE collaboration setup at intensities of $I = 4 \times 10^{15}$ W/cm², $I = 4 \times 10^{17}$ W/cm²: (i) the collective motion of conduction band electrons enhance the electric field while contributing to the absorption of laser light [14]. (ii) the high number of oscillating electrons in the nanorod accelerate those protons, which are close to the surface of the

nanorod, Fig. 1. (iii) the large density electron screening contributes for lowering the Coulomb barrier, phenomena present in stars as well [15].

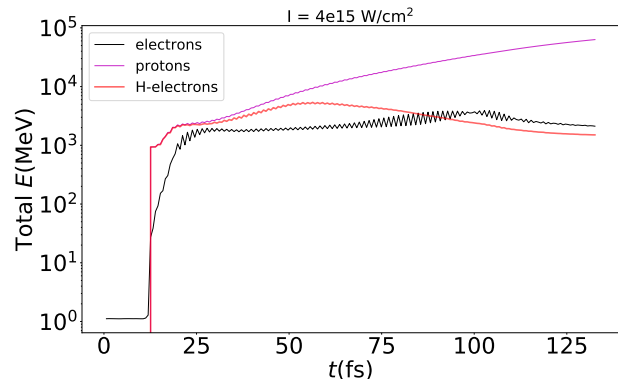


FIG. 2. (color online) We consider a laser pulse of intensity $I = 4 \cdot 10^{15}$ W/cm² and duration of 106fs. Here we show the time dependence of the total y directed energy of the conducting electrons in the nanorod (black line), protons resulting from ionization (magenta line) and Hydrogen electrons remaining from ionization (red line). It is shown that at 10 fs the laser light starts ionising the Hydrogen atoms, while at the same time the Hydrogen-electrons follow the collective motion of the gold nanorod electrons. The protons follow the same periodic motion with a phase delay.

Let us consider resonant nano-rod antennas embedded in Hydrogen rich polymer and/or with Hydrogen rich coating. The antennas are orthogonal to the direction of laser irradiation and are made of good plasmonic material with negative refraction index such as gold, or silver, or aluminum. Linear irradiation from two opposite directions, with electric field in phase is envisaged because in this case no net momentum is transferred to the nano-rods, but high energy is deposited to the antenna. The antenna should have the proper effective length in the given target and antenna materials and the length/diameter aspect ratio [25]. In this case the valence electrons will resonate between the two ends of the nano-rods due to the fluctuating in-phase electric field from the two laser beams. In case of sufficient intensity ($\approx 10^{17}$ W/cm²) of the laser beams the target material will be fully ionized, and its molecules will be fragmented to single atoms. (If the laser beam intensity is weaker molecules may fragment into groups and single atoms.) High Hydrogen content target materials or coatings will provide freely movable protons, which will be then accelerated due to the correlated motion of electrons and protons caused by the electric field strength on the nano-rod antennas. The large number of electrons in the nano-rod antennas (of length $\lambda_{eff} = 75-85$ nm) produce enormous field strength ($E_y = 3 \times 10^{12}$ V/m) [2], which may provide sufficient momentum for the smaller number of nearly 2000 times heavier protons.

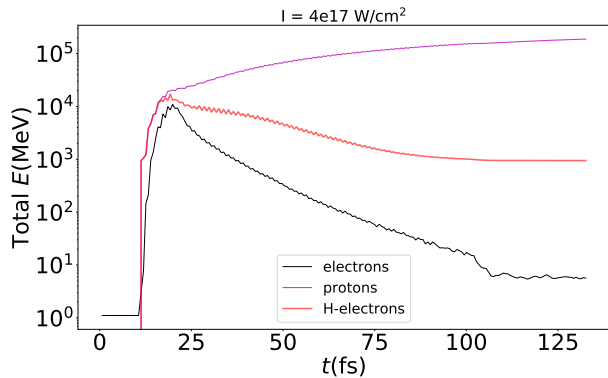


FIG. 3. (color online) We consider a laser pulse of intensity $I = 4 \cdot 10^{17} \text{ W/cm}^2$ and duration of 106fs. Here we show the time dependence of the total y directed energy of the conducting electrons in the nanorod (black line), protons resulting from ionization (magenta line) and Hydrogen electrons remaining from ionization (red line). It is shown that at 10 fs the laser light starts ionising the Hydrogen atoms, while at the same time the Hydrogen-electrons follow the collective motion of the gold nanorod electrons. The protons follow the same periodic motion with a phase delay.

This accelerator mechanism is similar to high energy particle accelerators where several electrode pairs with fluctuating electric charge accelerate the protons (e.g., in LHC in one pair of electrodes (cavity) the charges are about 10 cm apart and the potential is about 10^6 V/m. This is then repeated many times in a length of 27 km). One nano-rod antenna corresponds to one electrode pair in the particle accelerators. However, the electric field strength is six orders of magnitude higher, and the length of acceleration is six orders of magnitude shorter. These are estimates based on the EPOCH PIC kinetic model [22, 23]. The number of electrons is decisive for this mechanism. Here quantum effects in atomic physics play an important role [24]. Although single electrons are fermions they cannot be at the same place and time, but they can form pairs or other even number of collective quantum structures forming a Bose condensate. This enables correlated collective effects of large number of electrons.

II. DESCRIPTION OF THE MODEL AND METHODOLOGY

Plasmons on such nano antennas are usually studied theoretically by solving Maxwell's equations in simulations involving finite element or finite difference time-domain methods. These approaches are efficient for computers, however, some of the important phenomena are either neglected this way, or included typically by extra fitting parameters. The motion of free electrons is only

taken into account indirectly via the bulk permittivity of the metal. Classical methods using the dielectric function of the free electron gas: $\epsilon(\omega) = 1 - \omega_p^2/(\omega^2 + i\gamma\omega)$ with ω_p being the plasma frequency [21], neglecting electron-electron interactions. These interactions are mimicked by using an effective mass for the electrons. Here, γ is the collision frequency, prevalent in the damping constant in the above formula. Particle simulations on the other hand use the electron number density, n_e , to randomly distribute electron-like marker particles on the metal surface.

For our simulations we apply the Particle-in-Cell (PIC) method [27]. In PIC codes marker-particles (representing large number of real particles) move in continuous phase space, whereas densities and currents are computed in stationary mesh cells. We used the EPOCH multi-component PIC code [28]. This approach proved to be efficient for analyzing the electron dynamics in different plasmon modes, and modeling electron spill-out effects [29].

Two simulations were performed. (1) We examined the electron screening effect on a thin layer of proton "coating" surrounding the resonant nano antenna with density of 6.5×10^{28} proton/ m^3 . In the experiments the nanorod has a Dodecanethiol (DDT) capping: $\text{CH}_3(\text{CH}_2)_{11}\text{SH}$. This molecule is 1.3 nm long, with molar mass 202.39 g/mol and density of 0.845 g/ cm^3 . The thickness of the layer covering the nanorod is smaller than this, as the molecules bind to the surface at a certain angle. The attachment of these self-organized molecular monolayers to gold surfaces has been studied by many, and the literature has a wide range of data on coverage and angles for various cases [30]. The densest conformation only occurs on a perfectly (111)-oriented surface (111 here refers to the plane of atoms in a crystal described the Miller indices [33]). This was not taken into account, the resolution of the simulation box was greater than the size of this molecule.

(2) We inserted the nano antenna in a box filled neutral Hydrogen atoms with density of 4.27×10^{27} atoms/ m^3 (close to liquid density), in the limit where we can still treat every marker particle species participating as a plasma with kinetic approach. The Hydrogen atom consisted of 3 particle species: neutral Hydrogen atom, which could be ionised with the laser or by collisional ionization [32], protons and electrons resulting from the ionization. Furthermore, the gold nanorods consisted of 2 species: stationary Au^{3+} ions, and the moving conduction electrons.

Since the nanorod in our model calculation is 85 nm long and its diameter is $D = 25$ nm it has many different oriented surfaces thus one may only be able to estimate the coverage. We considered 3 electrons in the conduction band. Irradiation was done by 4×10^{15} W/ cm^2 and 4×10^{17} W/ cm^2 intensity plane wave, at 795 nm wave length, and pulse duration of 106 fs, just like in previous works [22, 23]. Similarly we were irradiating a calculation box (CB) of cross section $S_{CB} = 530 \cdot 530 \text{ nm}^2 = 2.81 \cdot 10^{-9}$

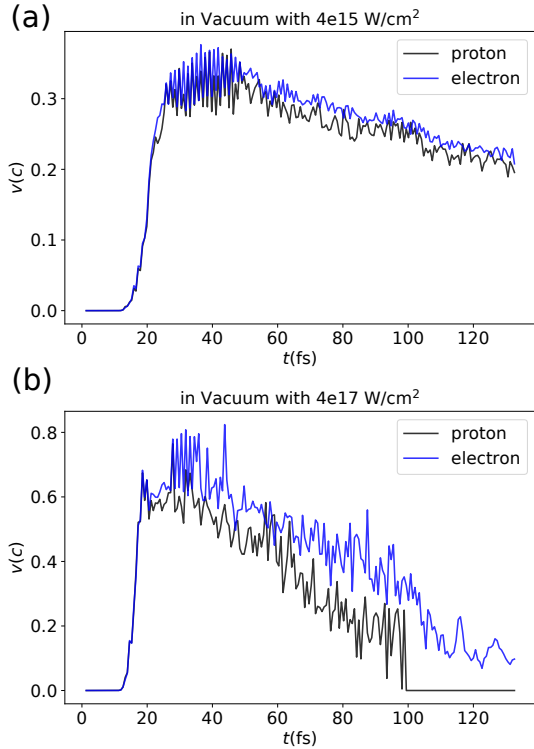


FIG. 4. (color online) We consider a laser pulse of intensity $I = 4 \cdot 10^{15} \text{W/cm}^2$ (a), $I = 4 \cdot 10^{17} \text{W/cm}^2$ (b), and duration of 106fs. These intensities are indicated in the figures as 15W/cm^2 (a), and 17W/cm^2 (b) respectively. Here we show in Vacuum the time dependence of the maximum velocity in y direction of the conducting electrons in the nanorod (black line), and of the surrounding protons resulting from ionization of Hydrogen (black line). Initially the electron and proton velocities are nearly the same indicating that the electrons are pulling the protons, which follow them. At the higher intensity (b), the initial electron and proton velocities about are twice as high. It is noticeable that the protons follow the collective motion of the plasmon electrons as long as the plasmonic effect is still alive. Once the number of electrons disappear through the electron spill-out, the protons will move in opposite direction. The number of protons will also be reduced at higher energies, as they are leaving the simulation box.

cm^2 and of length $L_{CB} = \lambda = 795 \text{ nm}$. The volume of CB being $0.2233 \mu\text{m}^3$, the total volume of H would be $V_{CB} - V_{nanorod}$, where $V_{nanorod} = 85 \cdot \pi \cdot (D/2)^2 = 41724.27 \text{ nm}^3$.

As the Hydrogen atoms are ionized, the number of neutral H marker particles in the simulation box decreases and proton and electron marker particles take their places. The leaving electrons from the ionization in the close vicinity, coupled to the plasmonic electrons through the laser, enhance further the accelerating effect on the protons at both laser intensities (see Figures 2, 3). This effect further increases the proton's momentum. see Fig. 2.

As seen in Fig. 2, the electro-magnetic field drives

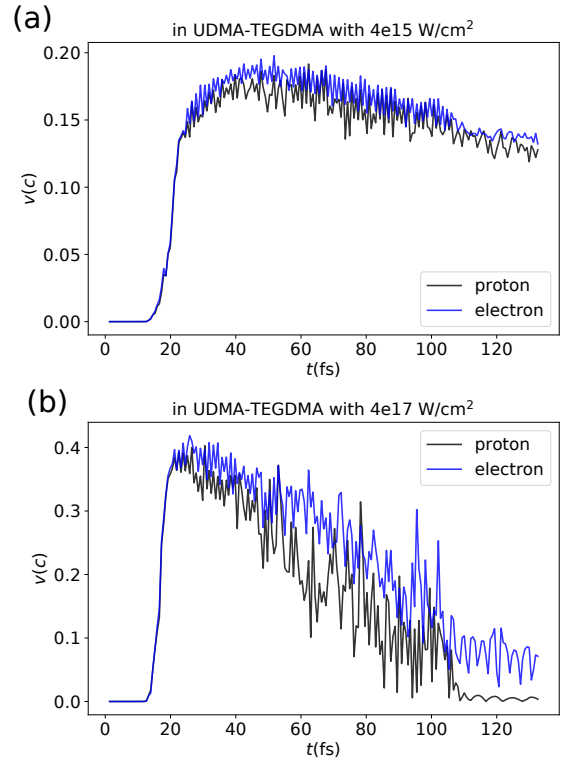


FIG. 5. (color online) Here we show the same emission data as in Fig. 4 in UDMA-TEGDMA polymer target for the same two laser beam intensities (a) and (b). In the polymer target the time dependence of the maximum velocity in y direction is reduced nearly to half of the value in vacuum for both the conducting electrons in the nanorod (black line), and of the surrounding protons resulting from ionization (black line). It is noticeable that the protons follow the collective motion of the plasmon electrons with the same velocity as long as the plasmonic effect holds. In the polymer the emission of electrons and protons lasts somewhat longer, showing that the polymer surrounding keeps the electrons longer in the nanorod antennas. Once the number of electrons disappear through the electron spill-out, the protons will move in opposite direction, however, this effect comes later than in Vacuum and much less intensely. The number of protons will also be reduced at higher energies, also leaving the simulation box, but slightly later than in the case of vacuum.

the conduction electrons into resonant fluctuations. In case of long irradiation times, $T_{pulse} \gg T$, our model describes a stationary configuration, adequate for gentle acceleration and compression. This would precede the short and extremely energetic ignition pulse in a Laser Wake Field Collider configuration [34]. At the transition from gentle irradiation to a few fs short ignition the nano antennas must not be destroyed. The solid state structure of the nano antennas would be destroyed when a significant part of the electrons left the nano antennas. This process takes a few ns, sufficient for the amplified ignition [34].

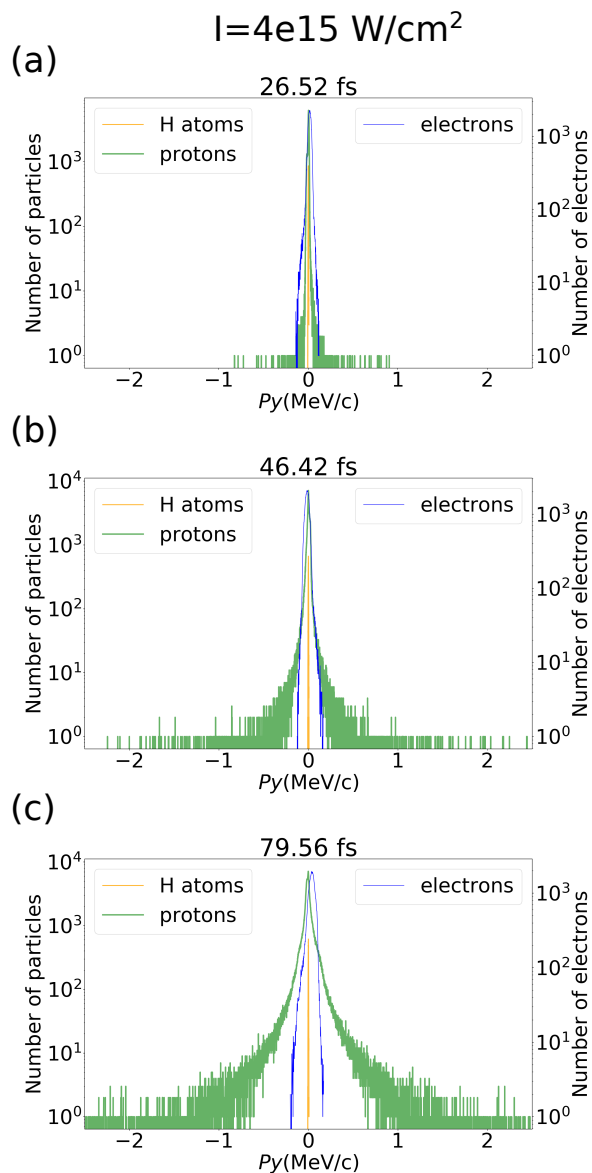


FIG. 6. (color online) The number of electrons and protons when they leave the nano antennas or their surrounding at intensity $I = 4 \times 10^{15} \text{ W/cm}^2$. Here we show the momentum distribution of particles at different times (a) 26.5 fs, (b) 46.42 fs, (c) 79.56 fs. The number of protons reaching high momentum ($P_y \geq 1 \text{ MeV/c}$) and 79.56 fs is small, while above $P_y \geq 500 \text{ keV/c}$ we have more than 10 protons, which is increasing exponentially with decreasing proton momentum. These proton energies are already sufficient for initiating nuclear reactions.

Note that for in medium simulations the speed of light, as well as the wave lengths are reduced by the refractive index to $c^* = c/n$ and $\lambda^* = \lambda/n$. Consequently in a dielectric medium like Urethane Dimethacrylate (UDMA) the resonant antenna length is reduced by n also, and further reduced by the "thick" aspect ratio (25:75) cf.

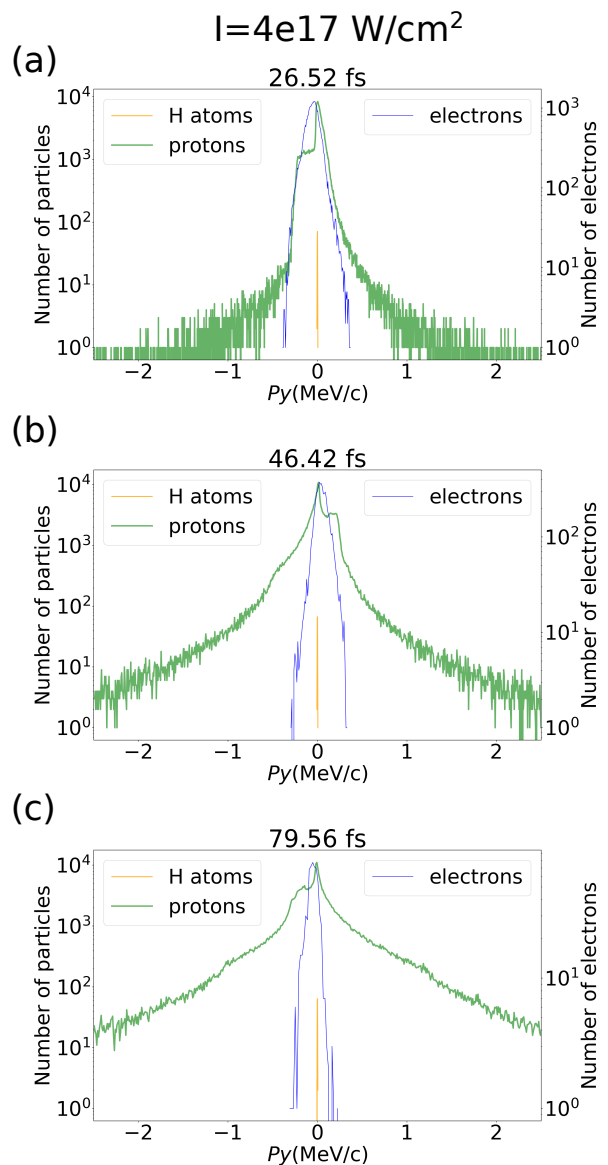


FIG. 7. (color online) The number of electrons and protons when they leave the nano antennas or their surrounding at intensity $I = 4 \times 10^{17} \text{ W/cm}^2$. Here we show the momentum distribution of particles at different times, similar properties are observable as in Fig.6, however much more protons reach higher energies as one would expect.

ref. [14]. See also the introductory comments based on ref. [25].

III. CONCLUSIONS

Compared to the classical particle accelerators like the LHC where the potential difference between the neighbouring RF cavities is $\sim 5 \cdot 10^6 \text{ V/m}$, here between the two ends of the resonant nano antennas is

$\sim 2 \cdot 10^{12} - \cdot 10^{13}$ V/m. [22, 23, 34] At the LHC this field accelerates protons between the RF cavities on a ~ 12.5 cm length, while by using resonant nano antennas the length of acceleration is 70 - 100 nm. At LHC the beam acceleration takes about 20 minutes and a million rotation in 27 km length, we have a 20 - 30 μm target thickness and 50-100 fs laser pulse length. Of course at LHC one accelerates about 10^{11} protons per bunch, while at the presently used laser facility at Wigner RCP with max laser beam pulse energy of 30 mJ, we estimate 10 protons at $P_y = 0.5$ MeV/c and 100 protons at $P_y = 0.5$ MeV/c.

At the high contrast Sylos laser facility, ELI-ALPS Szeged, Hungary, with higher laser beam intensity we expect to have protons at higher MeV energies and/or significantly larger proton numbers.

The model presented in this paper is idealized, but gives another possibility for us to capture the behavior of plasmonic nanorods on a small scale. Most importantly this kinetic model simulation has demonstrated that the collective effect of a large number of electrons can achieve a coherent proton acceleration. With proper target configuration this effect can be still multiplied.

The mechanism of the accelerating effect of the plasmonic electrons is more visible at smaller intensity (Fig. 2) due to less electron spill-outs leading to longer plasmon lifetime. The Hydrogen gets ionized and the protons and electrons get accelerated after the collective motion has reached to near field enhancement. This can be observed on Fig. 2 with the transition from the plateau to increase in the average energy. On Fig. 3 that transition is not observed due to faster response from the conducting electrons reaching higher momentum and dragging the protons and shorter plasmonic lifetime.

There are numerous theoretical predictions for Low Energy Nuclear Reactions. However, we have still to experimentally verify how these could be realized at higher energies, and what reaction rates can be achieved.

ACKNOWLEDGMENTS

Enlightening discussions with Johann Rafelski are gratefully acknowledged. Horst Stöcker acknowledges the Judah M. Eisenberg Professor Laureatus chair at Fachbereich Physik of Goethe Universität Frankfurt. We would like to thank the Wigner GPU Laboratory at the

Wigner Research Center for Physics for providing support in computational resources. This work is supported in part by the Frankfurt Institute for Advanced Studies, Germany, the Eötvös Loránd Research Network of Hungary, the Research Council of Norway, grant no. 255253, and the National Research, Development and Innovation Office of Hungary, via the projects: Nanoplasmonic Laser Inertial Fusion Research Laboratory (NKFIH-468-3/2021), Optimized nanoplasmonics (K116362), and Ultrafast physical processes in atoms, molecules, nanostructures and biological systems (EFOP-3.6.2-16-2017-

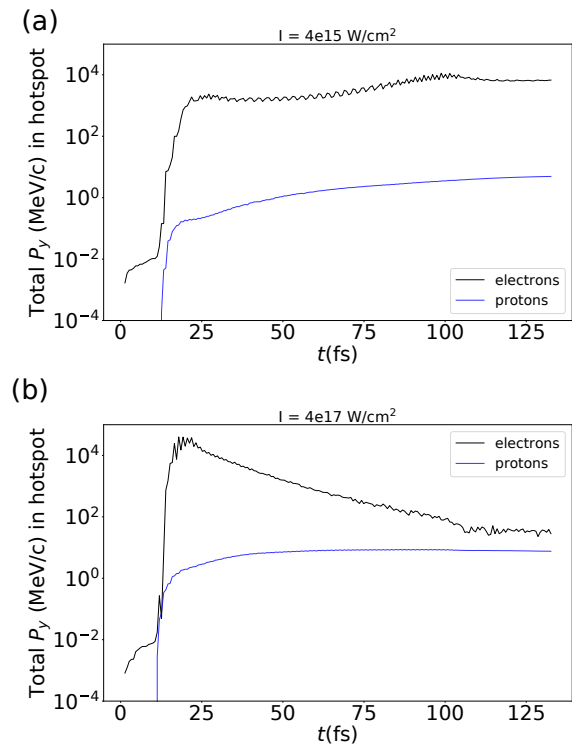


FIG. 8. (color online) Here we show the total momentum in the hotspots of the nanorod (typically 40 nm from the edges). (a) is at lower intensity of $4e15$ W/cm², (b) intensity of $4e17$ W/cm²

00005).

[1] L.P. Csernai, M. Csete, I.N. Mishustin, A. Motorenko, I. Papp, L.M. Satarov, H. Stöcker & N. Kroó, Radiation-Dominated Implosion with Flat Target, *Physics and Wave Phenomena*, **28** (3) 187-199 (2020). (arXiv:1903.10896v3).
 [2] S. Chandrasekhar, Hydrodynamic and Hydromagnetic Stability, *Oxford U. Press*, (1961).

[3] Kilkenny, J. D., Glendinning, S. G., Haan, S. W., Hammel, B. A., Lindl, J. D., Munro, D., Remington, B. A., Weber, S. V., Knauer, J. P., & Verdon, C. P. (1994). A review of the ablative stabilization of the Rayleigh-Taylor instability in regimes relevant to inertial confinement fusion. *Physics of Plasmas*, **1**(5), 1379-1389.
 [4] W. H. Cabot and A. W. Cook, Reynolds Number Effects on Rayleigh-Taylor Instability With Possible Im-

- lications for Type-1a Supernovae, *Nature Phys.* **2**, 252 (2006).
- [5] L.P. Csernai, Detonation on Timelike Front for Relativistic Systems, School of Physics, University of Minnesota, Minneapolis, Minnesota, USA, *Zh. Eksp. Teor. Fiz.* **92**, 397-386 (1987), & *Sov. Phys. JETP* **65**, 219 (1987).
- [6] L.P. Csernai, & D.D. Strottman, Volume Ignition via Time-Like Detonation in Pellet Fusion, *Laser and Particle Beams* **33**, 279-282 (2015).
- [7] L.P. Csernai, N. Kroó, & I. Papp, Radiation-Dominated Implosion with Nano-Plasmonics, *Laser and Particle Beams* **36**, 171-178 (2018).
- [8] Energy Increase in Multi-MeV Ion Acceleration in the Interaction of a Short Pulse Laser with a Cluster-Gas Target, Y. Fukuda, A. Ya. Faenov, M. Tampo, T. A. Pikuz, T. Nakamura, M. Kando, Y. Hayashi, A. Yogo, H. Sakaki, T. Kameshima, A. S. Pirozhkov, K. Ogura, M. Mori, T. Zh. Esirkepov, J. Koga, A. S. Boldarev, V. A. Gasilov, A. I. Magunov, T. Yamauchi, R. Kodama, P. R. Bolton, Y. Kato, T. Tajima, H. Daido, and S. V. Bulanov, *Phys. Rev. Lett.* **103**, 165002 (2009).
- [9] Gas-cluster targets for femtosecond laser interaction: Modeling and optimization, A. S. Boldarev, V. A. Gasilov, A. Ya. Faenov, Y. Fukuda and K. Yamakawa, *Rev. of Sci. Instruments*, **77**, 083112 (2006).
- [10] Measurements of D-D fusion neutrons generated in nanowire array laser plasma using Timepix3 detector, Peter Rubovic, Aldo Bonasera, Petr Burian, Zhengxuan Cao, Changbo, Fu, Defeng Kong, Haoyang Lan, Yao Lou, Wen Luo, Chong Lv, Yugan Ma, Wenjun Ma, Zhiguo Ma, Lukas Meduna, Zhusong Mei, Yesid Mora, Zhuo Pan, Yinren Shou, Rudolf Sykora, Martin Veselsky, Pengjie Wang, Wenzhao Wang, Xueqing Yan, Guoqiang Zhang Jiarui Zhao, Yanying Zhao, Jan Zemlicka, *Nuclear Instruments and Methods in Physics Research, Section A: Accelerators, Spectrometers, Detectors and Associated Equipment*, **985**, 2021, 164680 (2021).
- [11] High aspect ratio nanoholes in glass generated by femtosecond laser pulses with picosecond intervals, Sanghoon Ahn, Jiyeon Choi, Jiwhan Noh, Sung-Hak Cho, *Optics and Lasers in Engineering* **101**, 85-88 (2018).
- [12] M. Barbarino, Fusion reactions in laser produced plasma, PhD thesis, Texas A&M University (2015).
- [13] G. Zhang, M. Huang, A. Bonasera, Y. G. Ma, B. F. Shen, H. W. Wang, J. C. Xu, G. T. Fan, H. J. Fu, H. Xue, H. Zheng, L. X. Liu, S. Zhang, W. J. Li, X. G. Cao, X. G. Deng, X. Y. Li, Y. C. Liu, Y. Yu, Y. Zhang, C. B. Fu, and X. P. Zhang, Nuclear probes of an out-of-equilibrium plasma at the highest compression, *Phys. Lett. A* **383** (19), 2285-2289 (2019).
- [14] M. Csete, A. Szenes, E. Tóth, D. Vass, O. Fekete, B. Bánhelyi, I. Papp, T. S. Biró, L. P. Csernai, N. Kroó (NAPLIFE Collaboration), Comparative study on the uniform energy deposition achievable via optimized plasmonic nanoresonator distributions, *Plasmonics* **17** (2), 775-787 (2022).
- [15] Aliotta Marialuisa, Langanke Karlheinz, Screening Effects in Stars and in the Laboratory. *Frontiers in Physics*, vol. **10** (2022)
- [16] A. Bonyár et al., (NAPLIFE Collaboration), Nanoplasmonic Laser Fusion Target Fabrication - Considerations and Preliminary Results, Int. Conf. on New Frontiers in Physics, Kolymbari, Crete, Greece, Sept. 11, 2020.
- [17] M. Csete, et al. Plasmonic nanoresonator distributions for uniform energy deposition in active targets, *Optical Materials Express* **13**(1), 9-27 (2023).
- [18] Izabela M. Barszczewska-Rybarek Structure-property relationships in dimethacrylate networks based on Bis-GMA, UDMA and TEGDMA, *Dental Materials*, **25**(9), 1082-1089 (2009).
- [19] Bonyár A, Szalóki M, Borók A, Rigó I, Kámán J, Zangana S, Veres M, Rácz P, Aladi M, Kedves MÁ, Szokol Á, Petrik P, Fogarassy Z, Molnár K, Csete M, Szenes A, Tóth E, Vas D, Papp I, Galbács G, Csernai LP, Biró TS, Kroó N, NAPLIFE Collaboration, The Effect of Femtosecond Laser Irradiation and Plasmon Field on the Degree of Conversion of a UDMA-TEGDMA Copolymer Nanocomposite Doped with Gold Nanorods. *International Journal of Molecular Sciences* **23**(21), 13575 (2022).
- [20] K. Lance Kelly, Eduardo Coronado, Lin Lin Zhao, and George C. Schatz, *The Journal of Physical Chemistry B* **107** (3), 668-677 (2003).
- [21] S. A. Maier, Plasmonics: Fundamentals and Applications, New York, NY, *Springer Science & Business Media* (2007).
- [22] István Papp, Larissa Bravina, Mária Csete, Archana Kumari, Igor N. Mishustin, Dénes Molnár, Anton Motorenko, Péter Rácz, Leonid M. Satarov, Horst Stöcker, Daniel D. Strottman, András Szenes, Dávid Vass, Tamás S. Biró, László P. Csernai, and Norbert Kroó, (NAPLIFE Collaboration), Kinetic Model Evaluation of the Resilience of Plasmonic Nanoantennas for Laser-Induced Fusion, *PRX Energy*, **1**, 023001 (2022).
- [23] Papp István, Bravina Larissa, Csete Mária, Kumari Archana, Mishustin Igor N., Motorenko Anton, Rácz Péter, Satarov Leonid M., Stöcker Horst, Strottman Daniel D., Szenes András, Vass Dávid, Szokol Ágnes Nagyné, Kámán Judit, Bonyár Attila, Biró Tamás S., Csernai László P., Kroó Norbert, Kinetic model of resonant nanoantennas in polymer for laser induced fusion, *Frontiers in Physics*, **11**, 1116023 (2023).
- [24] Vladimir I. Vysotskii, Stanislav V. Adamenko, Mykhaylo V. Vysotskyy, Acceleration of low energy nuclear reactions by formation of correlated states of interacting particles in dynamical systems, *Annals of Nuclear Energy* **62**, 618-625 (2013).
- [25] Lukas Novotny, Effective Wavelength Scaling for Optical Antennas, *Phys. Rev. Lett.* **98**, 266802 (2007).
- [26] M. S. Dresselhaus, Solid State Physics - Part II Optical Properties of Solids, MIT Lecture Notes, (2001).
- [27] F. H. Harlow, Hydrodynamic Problems Involving Large Fluid Distortions, *J. Assoc. Comput. Mach.* **4**, 137 (1957).
- [28] T. D. Arber, et. al. Contemporary particle-in-cell approach to laser-plasma modelling, *Plasma Phys. Control. Fusion* **57**, 113001 (2015).
- [29] W. J. Ding, J. Z. J. Lim, H. T. B Do, et al. Particle simulation of plasmons *Nanophotonics*, **9**(10) 3303-3313 (2020).
- [30] L. Müller-Meskamp, B. Lüssem, S. Karthäuser, R. Waser, Rectangular ($3 \times 2\sqrt{3}$) Superlattice of a Dodecanethiol Self-Assembled Monolayer on Au(111) Observed by Ultra-High-Vacuum Scanning Tunneling Microscopy, *The Journal of Physical Chemistry B* **109**, 11424-11426 (2005).

- [31] K. Nanbu, S. Yonemura. Weighted particles in coulomb collision simulations based on the theory of a cumulative scattering angle. *Journal of Computational Physics*, **145**, 639–654 (1998).
- [32] F. Pérez, L. Gremillet, A. Decoster, M. Drouin, E. Lefebvre. Improved modeling of relativistic collisions and collisional ionization in particle-in-cell codes. *Physics of Plasmas*, **19**(8), 083104 (2012).
- [33] Neil W. Ashcroft, David N. Mermin, Solid state physics. New York: Holt, Rinehart and Winston (1976).
- [34] István Papp, Larissa Bravina, Mária Csete, Igor N. Mishustin, Dénes Molnár, Anton Motornenko, Leonid M. Satarov, Horst Stöcker, Daniel D. Strottman, András Szenes, Dávid Vass, Tamás S. Biró, László P. Csernai, Norbert Kroó, (NAPLIFE Collaboration) Laser Wake Field Collider; *Phys. Lett. A* **396**, 12724 (2021).
- [35] Makoto Shoji, Ken Miyajima, and Fumitaka Mafuné, Ionization of Gold Nanoparticles in Solution by Pulse Laser Excitation as Studied by Mass Spectrometric Detection of Gold Cluster Ions, *The Journal of Physical Chemistry C* **112** (6), 1929-1932 (2008).
- [36] Alberto Rivacoba, Electron spill-out effects in plasmon excitations by fast electrons, *Ultramicroscopy*, **207**, 112835 (2019).
- [37] M. Merschedorf, W. Pfeiffer, A. Thon, S. Voll, G. Gerber, Photoemission from multiply excited surface plasmons in Ag nanoparticles, *Appl. Phys. A* **71**, 547-552 (2000).
- [38] Gy. Farkas, Z.Gy. Horváth, Multiphoton electron emission processes induced by different kinds of ultrashort laser pulses, *Optics Comm.* **12** 392-395 (1974); Gy. Farkas, Z. Gy. Horváth, and Cs. Tóth Linear surface photoelectric effect of gold in intense laser field as a possible high-current electron source, *J. of Appl. Phys.* **62** 4545 (1987).
- [39] Archana Kumari, for the NAPLIFE Collaboration, LIBS Analysis of Pure, Deuterated and Au-doped UDMA-TEGDMA mixture: A Part of the Nanoplasmonic Laser Fusion Experiments, 11th Int. Conf. on New Frontiers in Physics 2022, Kolymbari, Crete, Greece, 7th Sept. (2022).
- [40] Miklós Veres, for the NAPLIFE Collaboration, Raman spectroscopic study of structural transformations in methacrylate polymer doped with plasmonic gold nanoparticles upon irradiation with high-energy femtosecond laser pulse, 11th Int. Conf. on New Frontiers in Physics 2022, Kolymbari, Crete, Greece, 7th Sept. (2022).
- [41] Norbert Kroó, for the NAPLIFE Collaboration, - invited talk - High field nanoplasmonics and some applications, Margaret Island Symposium 2022 on Vacuum Structure, Particles, and Plasmas, Budapest, May 15-18, (2022).
- [42] Péter Rácz, for the NAPLIFE Collaboration, - invited talk - LIBS spectra from polymer shootings, Margaret Island Symposium 2022 on Vacuum Structure, Particles, and Plasmas, Budapest, May 15-18, (2022).